

Arteriosclerosis, Thrombosis, and Vascular Biology



JOURNAL OF THE AMERICAN HEART ASSOCIATION

Human LDL Receptor Enhances Sequestration of ApoE4 and VLDL Remnants on the Surface of Hepatocytes but Not Their Internalization in Mice

Michael Altenburg, Jose Arbones-Mainar, Lance Johnson, Jennifer Wilder and Nobuyo Maeda

Arterioscler Thromb Vasc Biol. 2008;28:1104-1110; originally published online March 27, 2008;

doi: 10.1161/ATVBAHA.108.164863

Arteriosclerosis, Thrombosis, and Vascular Biology is published by the American Heart Association, 7272 Greenville Avenue, Dallas, TX 75231

Copyright © 2008 American Heart Association, Inc. All rights reserved.

Print ISSN: 1079-5642. Online ISSN: 1524-4636

The online version of this article, along with updated information and services, is located on the World Wide Web at:

<http://atvb.ahajournals.org/content/28/6/1104>

Data Supplement (unedited) at:

<http://atvb.ahajournals.org/content/suppl/2008/05/21/ATVBAHA.108.164863.DC1.html>

Permissions: Requests for permissions to reproduce figures, tables, or portions of articles originally published in *Arteriosclerosis, Thrombosis, and Vascular Biology* can be obtained via RightsLink, a service of the Copyright Clearance Center, not the Editorial Office. Once the online version of the published article for which permission is being requested is located, click Request Permissions in the middle column of the Web page under Services. Further information about this process is available in the [Permissions and Rights Question and Answer](#) document.

Reprints: Information about reprints can be found online at:

<http://www.lww.com/reprints>

Subscriptions: Information about subscribing to *Arteriosclerosis, Thrombosis, and Vascular Biology* is online at:

<http://atvb.ahajournals.org/subscriptions/>

Supplemental Materials for

Human LDL Receptor Enhances Sequestration of ApoE4 and VLDL Remnants on the Surface of Hepatocytes but not their Internalization in Mice

Michael Altenburg, Jose Arbones-Mainar, Lance Johnson, Jennifer Wilder, and Nobuyo Maeda

Department of Pathology and Laboratory Medicine, The University of North Carolina at Chapel Hill, Chapel Hill, North Carolina 27599-7525, USA

Detailed Methods

Quantitation of apoE and apoA1. ApoE and apoA1 content in lipoprotein fractions were quantified by an antigen capture enzyme-linked immunosorbent assay (ELISA), using a 1:10000 dilution of 1.5 mg/ml mouse monoclonal anti-human apoE antibody (Calbiochem) or rabbit anti mouse apoA1 antiserum (gift from Dr. H. deSilva) as described.¹

Adenoviruses. Plasmid vectors containing cytomegalus viral promoter-driven cDNA for fusion proteins, ApoE2-GFP, apoE3-GFP, and apoE4-GFP, were provided by Dr. Robert DeKroon at Duke University. These vectors express fusion proteins with EGFP (enhanced green fluorescent protein) attached to the C terminal end of each apoE isoform.² Adenoviral vectors encoding apoE2-GFP, apoE3-GFP, and apoE4-GFP were made using the AdEasy adenoviral system (Stratagene) according to the manufacturer's instructions. Ad-apoE-GFP's were amplified in 293 cells, purified by CsCl density gradient ultracentrifugation and dialyzed against 10 mM Tris pH 8.0, 2mM MgCl₂, 4% sucrose. Recombinant adenovirus stock stored at -80 °C was diluted with PBS and 1x10⁹ PFU in 0.2 ml of adenovirus was injected into a mouse via tail vein.

Culture of primary mouse hepatocytes. Mice were anesthetized using 2,2,2-tribromoethanol, the portal vein was cannulated with a 24-gauge plastic cannula, and the liver was perfused with Ca²⁺/Mg²⁺-free Hanks' Balanced Salt Solution containing glucose (10 mM) and HEPES (10 mM) at a flow rate of 3 ml/min for 10 min. The perfusion was continued for another 10 min with the same solution containing collagenase (0.05%, type I, Sigma). The liver was removed from the animal, minced in phosphate buffered saline (PBS), and the dissociated cells were dispersed by shaking followed by filtration through 100-µm nylon cell strainers (Falcon). The liver capsule and dish were rinsed in Dulbecco's modified Eagle's medium (DMEM) containing 0.02 µg/ml dexamethasone, 100 units/ml of penicillin and 100 µg/ml of streptomycin. The cells were pelleted by gravity sedimentation in Percoll for 5 min. at 4 °C. The medium was aspirated, leaving 5 ml total volume, and fresh medium was added to 10 ml. The cells were resuspended and viability was assessed by trypan blue exclusion. The yield of hepatocytes ranged from 3x10⁶ to 6x10⁶ cells/g of liver, and viability was greater than 80%. The cells were plated onto 60-mm mouse collagen IV-coated dishes (Falcon) at a density of 1.2x10⁶ viable cells/dish in 2 ml of the above medium containing 10% FBS unless otherwise stated.

Plasma lipoprotein analysis, DiI labeling and injection. Plasma was isolated and total cholesterol and triglycerides were measured as described.³ Pooled plasma samples (100 μ L) were fractionated by fast protein liquid chromatography (FPLC) using a Superose 6 HR10/30 column (Pharmacia Biotech Inc). The VLDL fraction was isolated from pooled plasma by ultracentrifugation at $d < 1.006$ g/ml and labeled with 1,1'-dioctadecyl-3,3,3',3'-tetramethylindocarbocyanine perchlorate (DiI C₁₈; Molecular Probes Inc.), as described by Stephan and Yurachek.⁴ DiI-labeled VLDL (100 μ g protein) was injected into tail veins of mice, and livers were fixed with 4% paraformaldehyde either 10 or 20 min later. DiI-labeled VLDL remaining in the plasma was determined using a microscope fluorometer (Olympus FV500 with a SPOT 2 digital camera) at 2min, 10 min, and 20 min using a modification of the fluorometric procedure described by Lorenze et al.⁵

Immunohistochemistry and confocal microscopic analyses. Animals were given a lethal overdose of 2, 2, 2-tribromoethanol. Livers were perfused through the portal vein at 2 ml/min for 2 min with 4% paraformaldehyde, excised from animals and further fixed overnight in 4% paraformaldehyde. Slides with consecutive liver paraffin sections (5 μ m) were incubated overnight at 4 °C with either goat anti-human apoE or goat anti-LDLR antibodies (1:1000, Calbiochem) followed by an incubation with FITC conjugated anti-goat IgG (1:500, Santa Cruz). Slides were cover slipped after application of Vectashield anti-fade mounting medium (Vector H-1000, Vector Laboratories) and were observed with an IX70 inverted microscope (Olympus) equipped with a filter set for FITC (exciter 560/55, dichroic 595, emitter 645/75, Chroma Technology Corp). Images were captured with a SPOT 2 digital camera (Diagnostic Instruments) and analyzed with SPOT version 4.0.9 (Diagnostic Instruments) and ImageJ 1.33u (NIH) software. For confocal microscopic analysis of apoE-GFP in fixed tissues, 50 or 100 μ m-thick sections were cut with a vibratome and stored free-floating in PBS at 4° C. Before analyses with an Olympus FV500 confocal microscope, individual sections were treated with sodium borohydride (1mg/ml in PBS) for 30 minutes at room temperature, and then washed in PBS three times for five minutes each at room temperature to reduce fixative-induced fluorescence. Individual vibratome sections were also stained with AlexaFluor633 labeled Wheat germ agglutinin (WGA) (50 micrograms/ml) for 30 min. For GFP fluorescence, the 488 line of an Argon laser was used for excitation and the 505 to 525 nm band-pass filter for emission. To acquire labeled WGA images for endothelial cell staining, the 633 line of a Helium/Neon-red laser was used for excitation and the 660 band-pass filter for emission (Cy5). GFP and Alexaflour633 fluorescence images were scanned independently with only their respective excitation and emission frequencies to eliminate bleed through. To acquire DiI labeled images for VLDL uptake, the 543 nm line of a Helium/Neon-green laser was used for excitation and the 560-600 band-pass filter for emission (DiI).

Gene Expression. RNA was extracted using RNAeasy kit (Qiagen, Valencia, CA) according to the manufacturer's protocol from livers of mice that were fed a HFW diet for 2 weeks. Real time RT-PCR amplifications were performed in a 96-well plate in the ABI Prism 7700 sequence detector (PE Biosystems) in a total volume of 30 μ l, which included 10 μ l of RNA sample from the ABI Prism 6700 plus 20 μ l of a reaction mixture. Each RT-PCR amplification was performed in duplicate: 30 min at 48 °C for the RT reaction and then 10 min at 94 °C, followed by a total of 40 temperature cycles (15sec at 94 °C and 1 min at 60 °C). To determine total *Ldlr* mRNA levels, a primer probe system specific for murine exon 1, which is also present in mice targeted for the *huLDLR*, was used.⁶

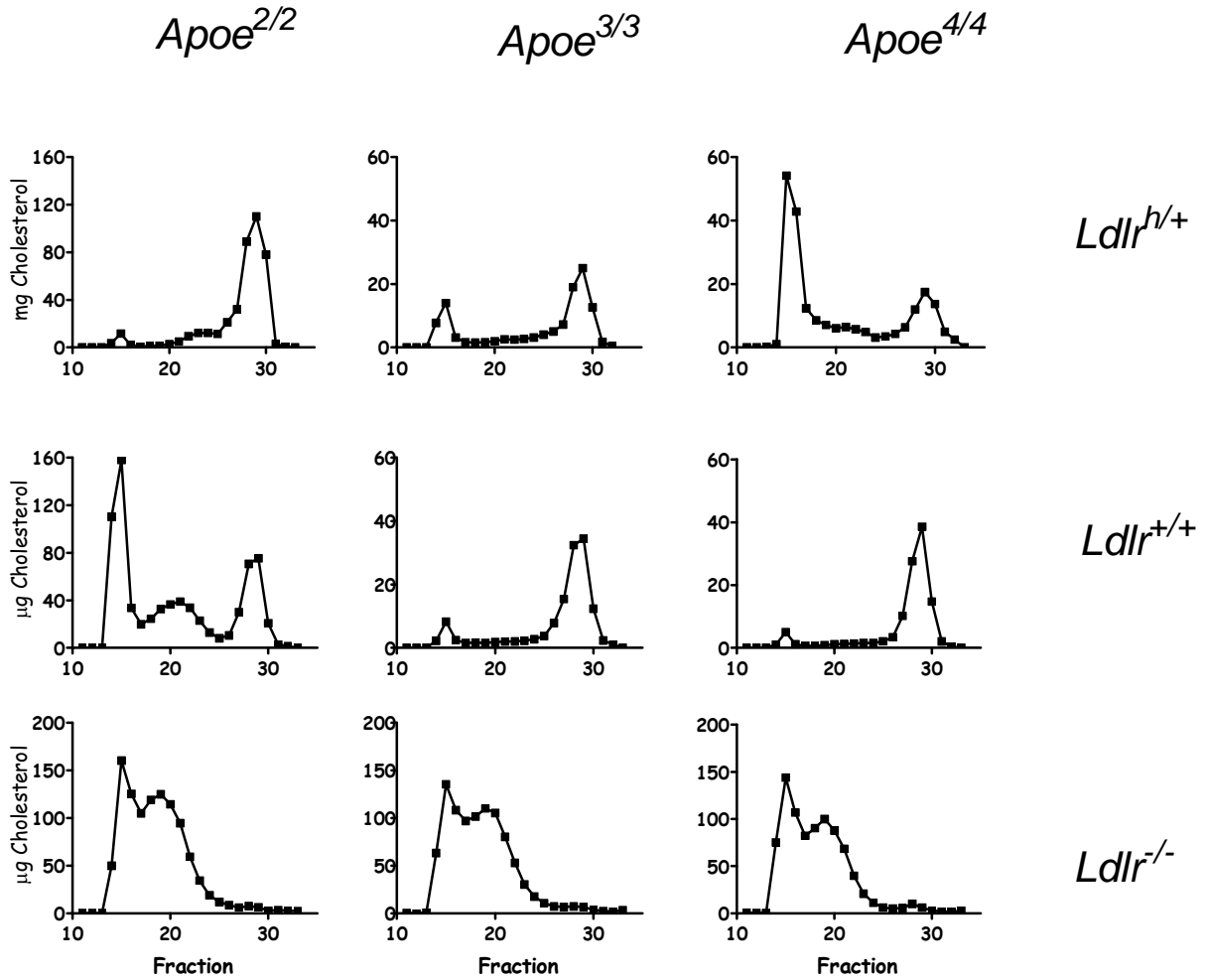
Liver membrane isolation and Western Blotting for LDLR. Livers were removed and transferred to 5 ml of an ice-cold solution of 0.25 M sucrose, 0.1 M Tris, and protease inhibitors (200mM PMSF, leupeptin, aprotinin), pH 7.4. The livers were homogenized and spun at $10000 \times g$ for 10 min to pellet cell debris and nuclei. The supernatant was centrifuged at $100,000 \times g$ for 30 min. The resulting membrane containing pellet was resuspended in 0.5 ml of Tris-buffered saline TBS with protease inhibitors, using a 22 gauge needle. The second supernatant was centrifuged again at $100,000 \times g$ for 30 min and the pellet was resuspended in 100ul of TBS. 10 μ g of protein as determined by Bradford Assay (Bio-Rad) was run on a 4-20% pre-cast gradient gel (NuSep) and transferred to an Immobilon –P membrane (millipore). Anti HuLDLR (Fitzgerald Industries International) and Anti Mouse LDLR (R&D systems) as well as horseradish peroxidase conjugated secondary antibodies were used at a 1:10000 dilution. After washing 4X 10 min in TBS-Tween, blots were developed with ECL reagent (Amersham) and exposed to Film (Kodak).

Heparin and Heparinase treatments and injections. Mice were injected via the tail vein with heparinase (30U/mouse; Sigma). Five min after heparinase injection mice, were injected via tail vein with 100 μ g DiI labeled Eko VLDL and blood was collected after 2, 5, 10, and 20 min. Primary hepatocytes were treated with 3U/ml Heparinase (Sigma) for 1hour.

Supplemental Table 1 Description of mice used in the work.

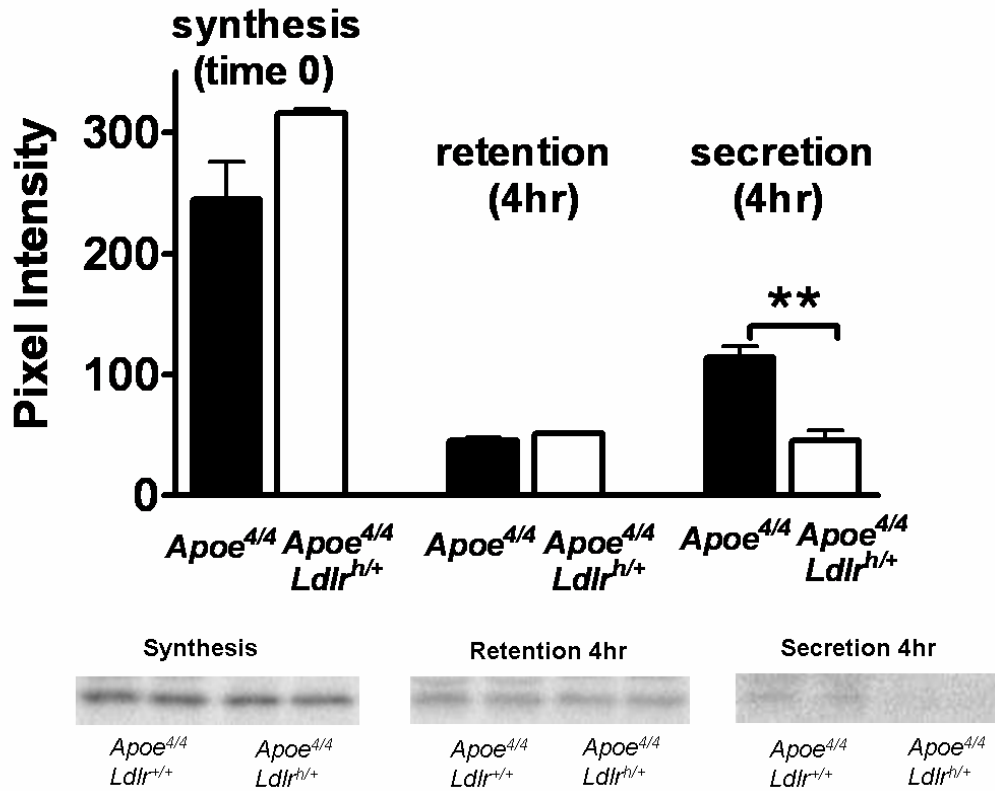
Supplemental Table 1		
Mice Genotype	Abb.	Description
<i>Apoe</i> ^{2/2}	2m	human apoE2 C57BL/6
<i>Apoe</i> ^{2/2} <i>Ldlr</i> ^{h/+}	2h	human apoE2 and increased LDLR C57BL/6
<i>Apoe</i> ^{3/3}	3m	human apoE3 C57BL/6
<i>Apoe</i> ^{3/3} <i>Ldlr</i> ^{h/+}	3h	human apoE3 and increased LDLR C57BL/6
<i>Apoe</i> ^{4/4}	4m	human apoE4 C57BL/6
<i>Apoe</i> ^{4/4} <i>Ldlr</i> ^{h/+}	4h	human apoE4 and increased LDLR C57BL/6
<i>Apoe</i> ^{4/4} <i>Ldlr</i> ^{-/-}	4ko	human apoE4 and no LDLR C57BL/6
<i>Apoe</i> ^{-/-}	Eko	no apoE C57BL/6
<i>Apoe</i> ^{-/-} <i>Ldlr</i> ^{h/h}	Eh	no apoE and increased LDLR (homozygous) C57BL/6
<i>Ldlr</i> ^{-/-}	ll	no LDLR C57BL/6
<i>Ldlr</i> ^{h/h}	hh	increased LDLR (homozygous) C57BL/6

Supplemental Figure I.



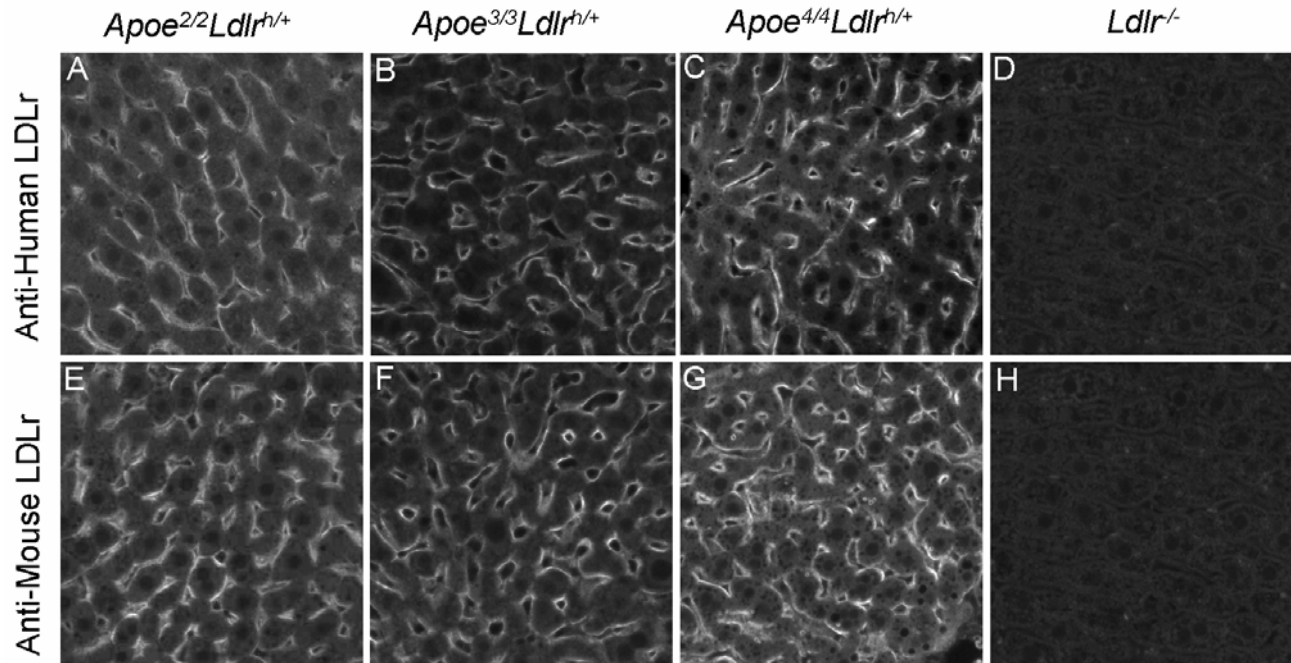
Supplemental Figure I. Lipoprotein distribution in mice with human apoE. Mice expressing apoE2 (left), apoE3 (center) and apoE4 (right) with no LDLR (*Ldlr*^{-/-}, bottom), wildtype (*Ldlr*^{+/+}, center), and overexpression of the LDLR (*Ldlr*^{h/+}, top) were on a HFW diet. Plasma lipoproteins were separated by FPLC and cholesterol in each fraction is shown. VLDL, fractions 14-16; LDL, fractions 19-23; HDL, fractions 26-30.

Supplemental Figure II.



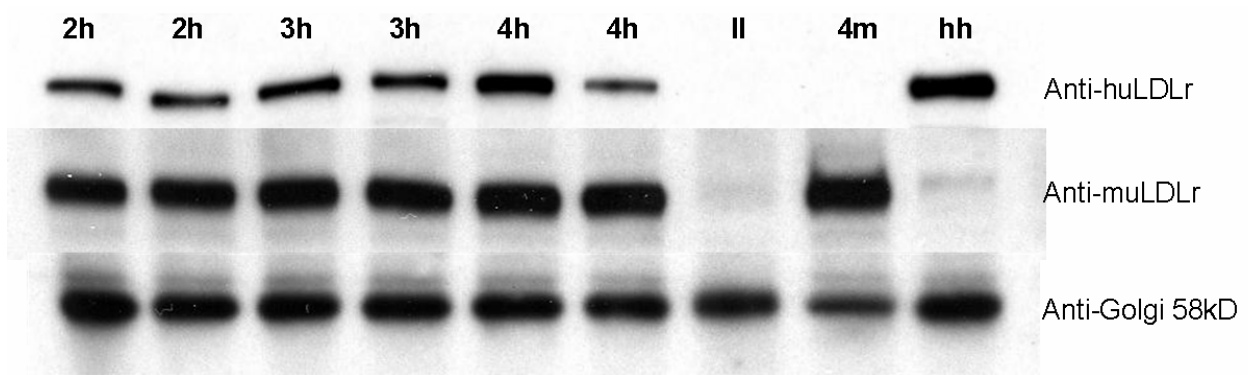
Supplemental Figure II. Pulse chase analysis of Apoe^{4/4} and Apoe^{4/4}Ldlr^{h/+} hepatocytes. Cell-associated apoE (synthesis, time 0) during a 60 min pulse and after a 4hr chase (retention) and apoE in medium (secretion) was immunoprecipitated and separated by SDS-PAGE. ³⁵S-Methionine in each band was measured using phosphoimager. Values shown are average of three wells. The experiment was repeated with a similar result. ** p≤0.005

Supplemental Figure III.



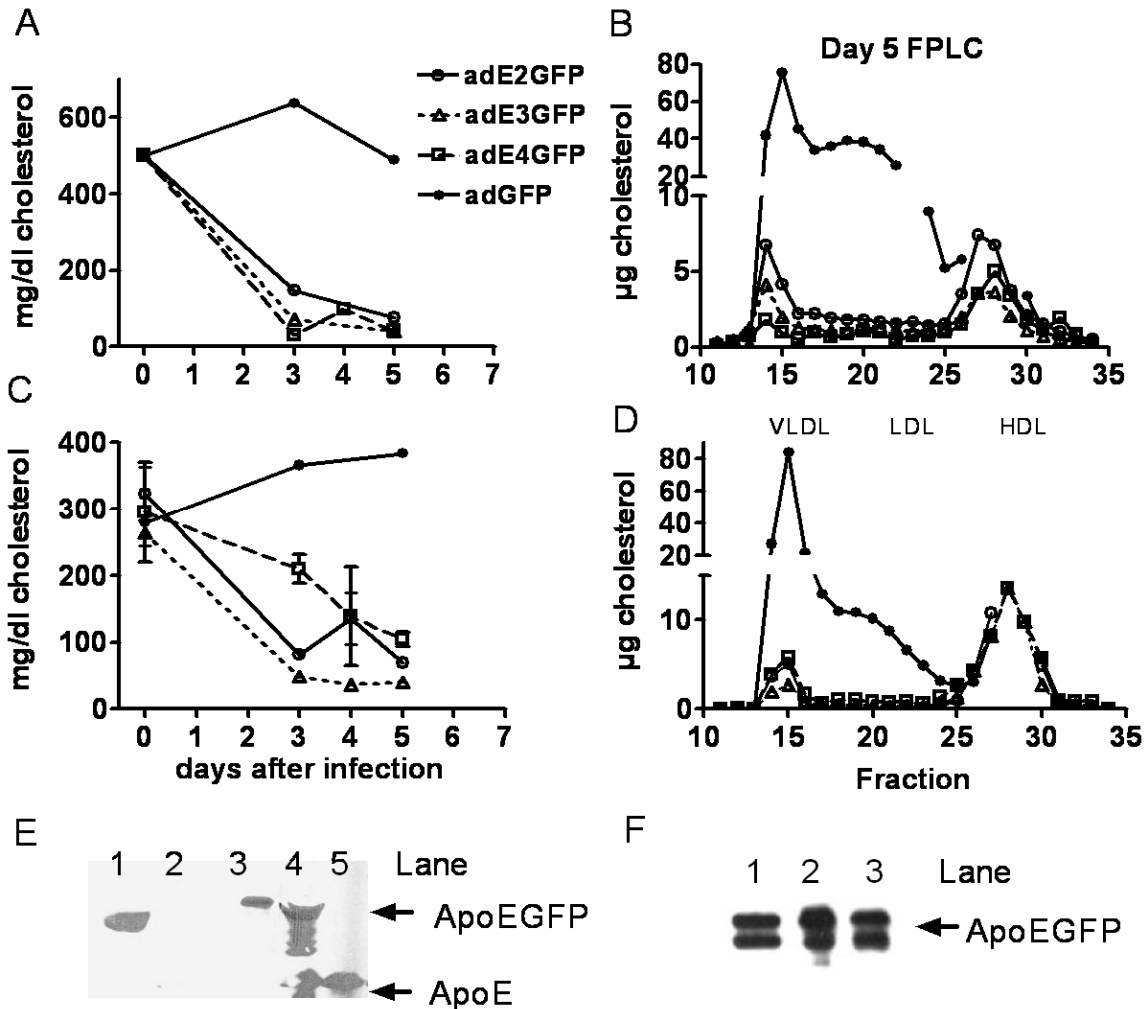
Supplemental Figure III. *Immunohistochemical localization of LDLR in the liver of mice.* Top row, Anti-human LDLR staining of (A) *Apoe^{2/2}Ldlr^{h/+}*, (B) *Apoe^{3/3}Ldlr^{h/+}*, (C) *Apoe^{4/4}Ldlr^{h/+}*, and (D) *Apoe^{4/4}Ldlr^{-/-}* liver. (A). Bottom row, staining for anti-mouse LDLR apoE in (E) *Apoe^{2/2}Ldlr^{h/+}*, (F) *Apoe^{3/3}Ldlr^{h/+}*, (G) *Apoe^{4/4}Ldlr^{h/+}*, and (H) *Apoe^{4/4}Ldlr^{-/-}* livers. (600X).

Supplemental Figure IV.



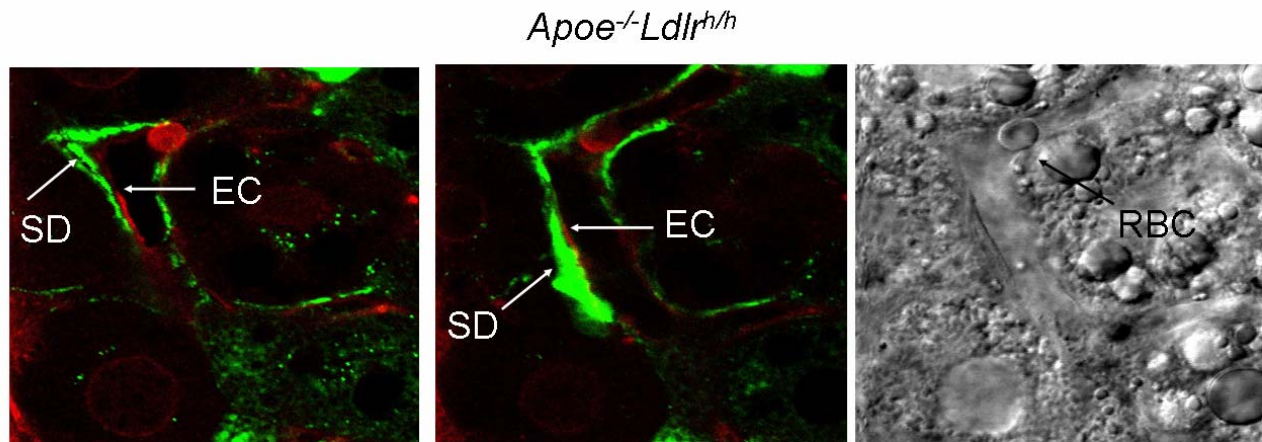
Supplemental Figure IV. *Liver membrane LDLR levels.* Western blots using antibodies specific for the human LDLR (top) and mouse LDLR (middle). 10 μ g protein of liver sample was loaded in each lane subjected to SDS-PAGE. An antibody to the membrane protein Golgi 58 KDa was used as a loading control (bottom). The 3 lanes furthest to the right (ll, 4m, hh) indicate the minimal cross-reactivity between anti-huLDLr with muLDLr, and anti-MuLDLr and huLDLr.

Supplemental Figure V.



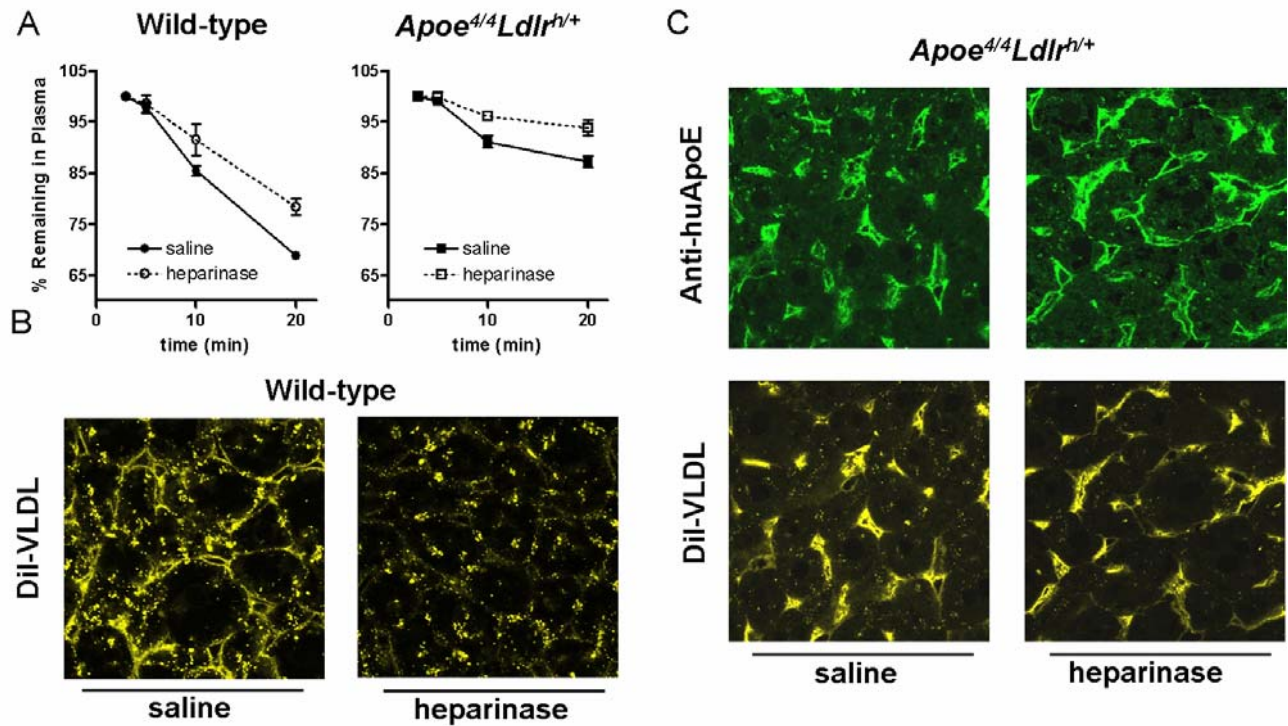
Supplemental Figure V. Effect of Ad-apoE-GFP on plasma lipid levels. Plasma cholesterol levels were monitored over 5 days in (A) the *Apoe*^{-/-} mice and (C) the *Apoe*^{-/-}*Ldlr*^{h/h} mice transfected with Ad-apoE2-GFP (black circles with solid line), Ad-apoE3-GFP (open triangles with dotted line), Ad-apoE4-GFP (black squares with dashed line), or Ad-GFP (black dots with solid line). Distribution of cholesterol among different lipoprotein fractions was assessed by FPLC of plasma samples at day 5 in (B) the *Apoe*^{-/-} mice and (D) the *Apoe*^{-/-}*Ldlr*^{h/h} mice. (E), Western blot of plasma from *Apoe*^{-/-} mice transfected with Ad-apoE3-GFP (lane 1) or without transfection (lane 2), VLDL isolated from Ad-apoE3-GFP transfected *Apoe*^{-/-} mice (lane 3), plasma of wild type C57BL/6J mice transfected with Ad-apoE3-GFP (lane 4) or without transfection (lane 5). (F), ApoE3-GFP associated with VLDL, LDL, and HDL separated by FPLC (fractions 15, 23 and 28, respectively, in panel B) from the *Apoe*^{-/-} mice transfected with Ad-apoE3-GFP. These data demonstrate that apoE-GFP fusion proteins are functional and appear to retain isoform-specific characteristics. Since apoE4-GFP can lower cholesterol when over-expressed by adenoviral vector in the liver of *Apoe*^{4/4}*Ldlr*^{h/h} mice, adverse effects of LDLR on plasma lipids must be dependent on the relative ratios between apoE4 and LDLR.

Supplemental Figure VI.



Supplemental Figure VI. *Localization of apoE4-GFP protein on the surface of hepatocytes.* Examination under a higher magnification (1500x) of the two consecutive images shows that apoE4-GFP in the sinusoidal space (SD) in the AdapoE4-GFP transfected *ApoE^{-/-}Ldlr^{h/h}* liver (green) is localized beneath the endothelial cell lining (EC) stained for lectin (red). Black arrow in the bright field indicates a red blood cell (RBC), which also stained red.

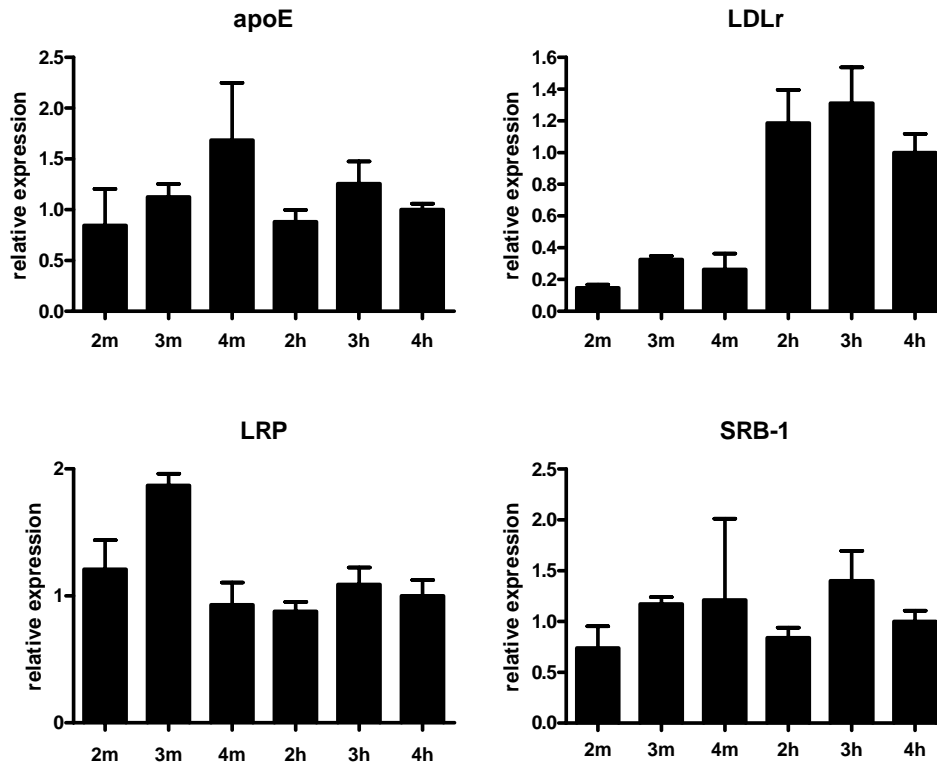
Supplemental Figure VII.



Supplemental Figure VII. *Heparinase effects on VLDL uptake by the liver.* Heparinase (30U/mouse) injected 5 min prior to subsequent injection of apoE^{-/-} DiI labeled VLDL. (A) Clearance of VLDL in wildtype mice (left) and in *Apoe^{4/4}Ldlr^{h/+}* mice plasma DiI-fluorescence at 2min was taken to be 100%. Both genotypes had a delay in VLDL clearance after heparinase. (B) DiI-fluorescence in wildtype liver 20 min after VLDL injection with saline (left) or heparinase (right). (C) Top panel, apoE immunostaining in 50 μm vibratome sections of *Apoe^{4/4}Ldlr^{h/+}* liver 20 min after VLDL injection with saline (left) or heparinase (right). (C) Bottom panel, DiI-fluorescence in *Apoe^{4/4}Ldlr^{h/+}* liver after saline (left) or heparinase (right).

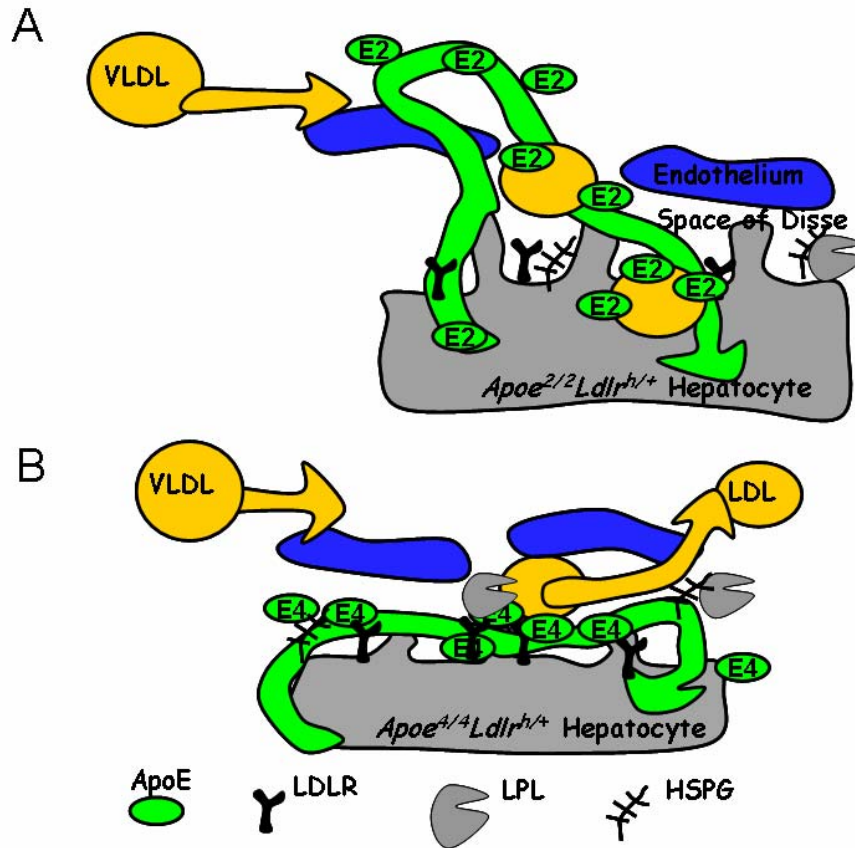
Supplemental Figure VIII

Gene Expression after HFW



Supplemental Figure VIII. Gene Expression in the liver. Relative mRNA levels of the genes were normalized by the expression of β -actin. Values are mean \pm S.E. and relative to 4h, which was adjusted to 1. Expressions of apoE, LRP, and SRB-1 were not significantly different among mice with different apoE isoforms. There was an expected increase in LDLR in mice that had the *ldl***h* allele compared to mice with wildtype *ldl*. Thus, the effect of apoE isoform on VLDL uptake does not appear to involve pathways affecting expression of apoE, LDLR, LRP, and SRB-1. $N > 4$ for each genotype.

Supplemental Figure IX.



Supplemental Figure IX. Hypothetical mechanism to explain the potential role of the apoE LDLR interaction on VLDL metabolism. Endothelial cells (blue) separate the hepatic sinusoid and plasma space from the space of Disse and hepatocyte microvilli (grey). (A) Top diagram shows apoE2 metabolism of apoE-poor VLDL. VLDL (yellow) that has yet to be enriched in apoE enters on the left. The lower LDLR affinity of apoE2 increases the circulation of plasma apoE level (green arrow), and apoE2 locates out of the space of Disse into the plasma. The elevated plasma apoE2 transfers onto VLDL (perhaps from other lipoproteins such as HDL, which is elevated in mice with apoE2). This increases the enrichment of apoE2 onto VLDL which then facilitates LDLR and HSPG mediated uptake without sequestration. (B). Lower diagram shows apoE4 metabolism of apoE-poor VLDL. The life cycle of apoE4 compared to apoE2 is more confined to the space of Disse (green arrow). High LDLR affinity of apoE4 keeps it bound to the hepatic surface, and plasma apoE4 levels are low. ApoE poor VLDL is not enriched with apoE in the plasma as is apoE2. These un-enriched apoE VLDL are stuck at the hepatic surface and are not internalized. The sequestering of VLDL on the surface exposes it to lipases and subsequently they are converted to remnants and LDL.

References

1. Arbones-Mainar JM, Navarro MA, Acin S, Guzman MA, Arnal C, Surra JC, Carnicer R, Roche HM, Osada J. Trans-10, cis-12- and cis-9, trans-11-conjugated linoleic acid isomers selectively modify HDL-apolipoprotein composition in apolipoprotein E knockout mice. *J Nutr.* 2006;136:353-359.
2. Dekroon RM, Armati PJ. Endocytosis of apoE-EGFP by primary human brain cultures. *Cell Biol Int.* 2002;26:761-770.
3. Knouff C, Briand O, Lestavel S, Clavey V, Altenburg M, Maeda N. Defective VLDL metabolism and severe atherosclerosis in mice expressing human apolipoprotein E isoforms but lacking the LDL receptor. *Biochim Biophys Acta.* 2004;1684:8-17.
4. Stephan ZF, Yurachek EC. Rapid fluorometric assay of LDL receptor activity by DiI-labeled LDL. *J Lipid Res.* 1993;34:325-330.
5. Lorenz JN, Gruenstein E. A simple, nonradioactive method for evaluating single-nephron filtration rate using FITC-inulin. *Am J Physiol.* 1999;276:F172-177.
6. Altenburg MK, Johnson LA, Wilder JC, Maeda N. Apolipoprotein E4 in macrophages enhances atherogenesis in an LDL receptor dependent manner. *J Biol Chem.* 2007.